LIST OF ABBREVIATIONS

ADC - Analog Digital Converter

EMR - Electromagnetic Radiation

GATT - Generic Attribute

GUI - Graphical User Interface

I2C - Inter-Integrated Circuit

ICNIRP - International Commission on Non-Ionizing Radiation

IEC - International Electrotechnical Commission

IMU - Inertial Measurement Unit

IP - Ingress Protection

RF - Radio Frequency

RoHS - Reduction of Hazardous Substances

RSSI - Received Signal Strength Indication

SAR - Specific Absorption Rate

4. EVALUATION

The following section contains the results of the individual subsystem tests as well as a test of the integrated system. Each design constraint was explicitly considered when designing the individual tests. Table 4.1 contains the technical constraints that were tested.

Table 4.1. Technical Design Constraints

Name	**Description**
Hand Orientation	The glove must determine the angles of wrist flexion, extension, and deviation within a ±3° margin of error. Also, the glove must measure wrist acceleration, hand orientation, and hand acceleration within a ±5% margin of error.
Wireless Communication	The wrist-mounted controller must communicate wirelessly with a range that will span the average width of a tee box: 9.15 m.
Data Display	The data is recorded and displayed at 120 Hz.
Unobtrusive	The user must not be obstructed while gripping the club with the glove on. The wrist-mounted controller must have a footprint smaller than the average sweat-band size of 7.62 cm. The sensor wires in the glove must not interfere with swing motion.
Portability	The minimum battery life of the system must exceed 5 hours of use.

Figure 4.1 displays the system overview.

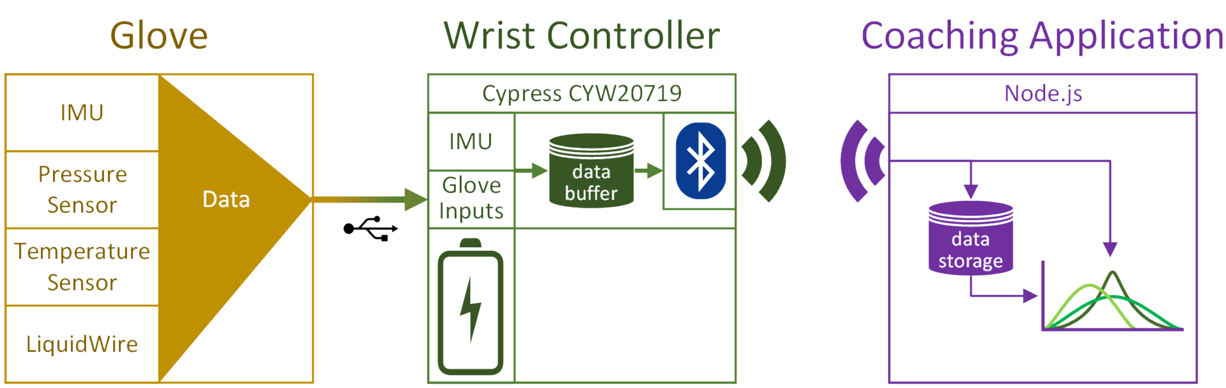

Figure 4.1. System Overview

4.1. Glove Subsystem

4.1.1. Accelerometer

The design is constrained to ±5% margin of error to ensure that the accelerometer records the user's hand precisely. To test the accelerometer, it was placed on the inside of a 3D printed cube with flat sides on every axis. The cube was placed on each of its three orthogonal sides and the values for X, Y, and Z acceleration were recorded in Table 4.1 below. The percent error for the dimension being tested is listed alongside the measured value. As seen, each sensor reading percent error fell within the required design constraint.

Table 4.1 Accelerometer Test

Test Axis	Expected (m/s^2)	Actual (m/s^2)	Error
X	9.8	10.050	2.5%
Y	9.8	9.786	0.14%
Z	9.8	10.135	3.4%

4.1.2. Gyroscope

The operation of the gyroscope was tested by rotating the test apparatus on each axis at a rate of 90° per 840 ms. At this rate, the expected degrees per second (dps) is 104.65. Table 4.2 lists this expected value and the value that was measured during the tests for each dimension. Once again, the percent error for each axis satisfied the design constraint of ±5% margin of error.

Table 4.2 Gyroscope Test

Test Axis	Expected (dps)	Actual (dps)	Error
X	104.65	102.417	2.13%
Y	104.65	101.726	2.79%
Z	104.65	103.129	1.45%

4.1.3. LiquidWire

The LiquidWire stretch sensors must meet the Hand Orientation technical constraint of measuring the user's wrist flexion and deviation to within 3° of error. To test the LiquidWire stretch sensors, a sensor was placed on a testing apparatus that emulates the motion of a wrist. This apparatus is seen in Figure 4.2. The lever was moved from its 90° resting position to the final resting position at 0° in 3° increments. The measurements from these increments are graphed in Figure 4.3. This graph shows a linear relationship between angle and resistance while exhibiting a measurable change in resistance between every 3° increment.

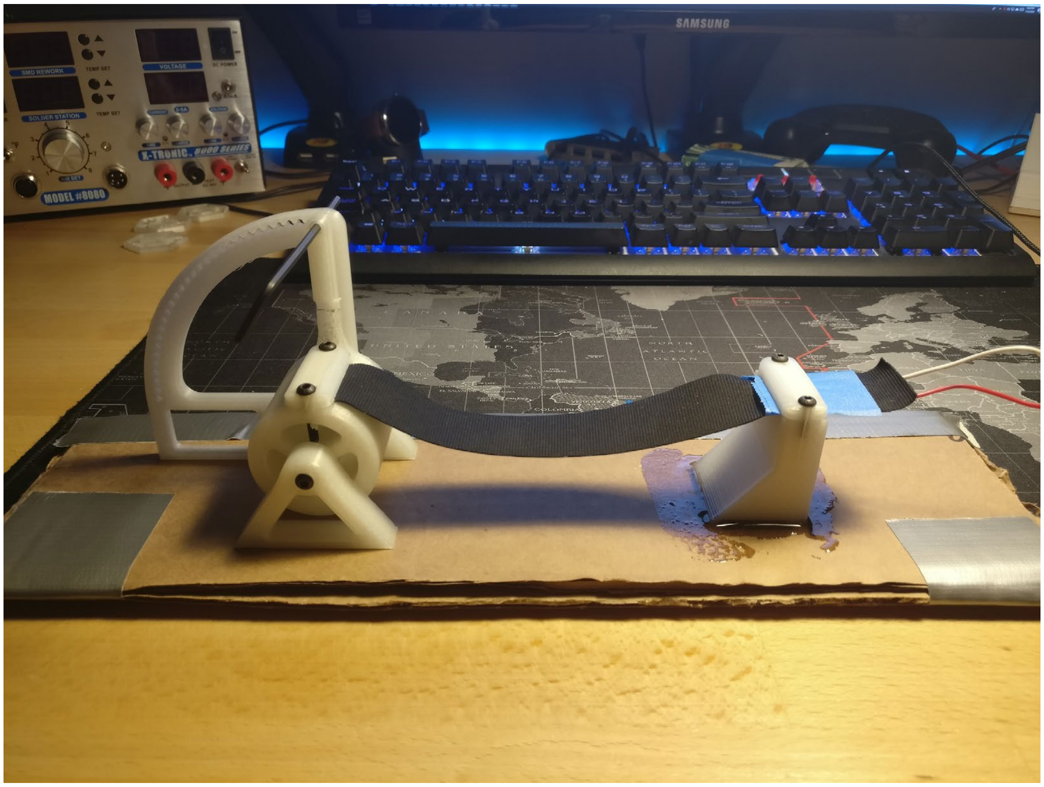

Figure 4.2. LiquidWire Test Apparatus

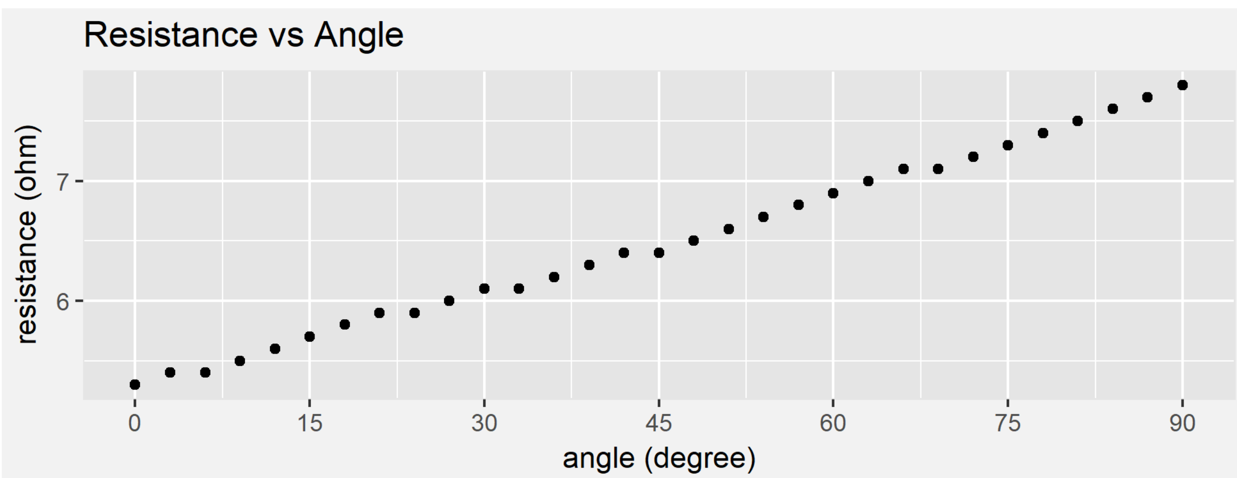

Figure 4.3. LiquidWire Test Measurements

4.1.4. Pressure Sensor

Finally, a pressure sensor was connected to a multimeter and placed onto a 50 kg scale. A container of water was placed on top of the pressure sensor. A 3D-printer adapter focused the force from the container onto the small face of the pressure sensor. Water was added in 1 kg increments and the resistance was recorded after each increment. Figure 4.4 displays measured and expected resistance values.

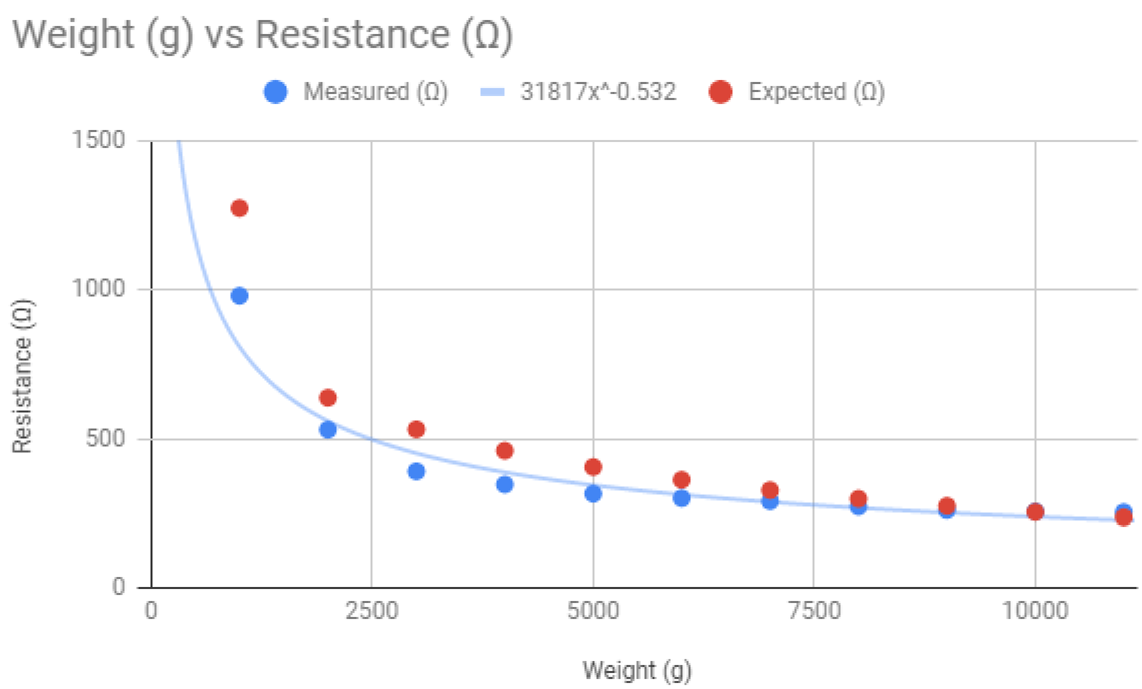

Figure 4.4. Pressure Sensor Test

4.2. Wrist-mounted Microcontroller Subsystem

4.2.1. Battery

The battery was tested using an Arduino, a voltage divider, and a 36 Ω resistor. The battery was fully charged to 4.2 V and connected across the voltage divider. The Arduino was programmed to measure, interpret, and display battery voltage values every 30 seconds. The 36 Ω resistor was attached to the leads of the battery to simulate an average current draw of 0.1 A. Once the battery was depleted, the values were stored and plotted in a Voltage vs. Time graph seen in Figure 4.5.

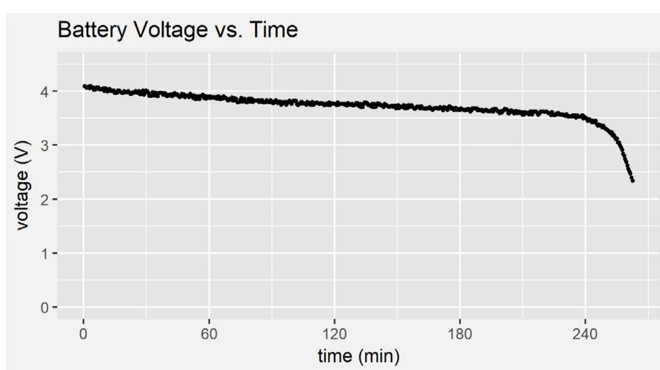

Figure 4.5. Battery Test

With an elapsed time of 4.375 hours and an average current draw of 0.103 A, the battery discharged 451.5 mAh over the duration of the test. Because the system will draw no more than 90 mA during peak usage, the battery is sufficient to meet the 5-hour runtime constraint.

4.2.2. Sensor Polling

To ensure proper operation of the I^2C bus, the first sensor test was to capture digital data transmission. The SDA and SCLK lines from the microcontroller were connected to the D0 and D1 inputs on a National Instruments Mixed Signal Oscilloscope. Next, a trigger was set for the oscilloscope output to trigger on the first data transfer. Figure 4.6 shows the oscilloscope output that depicts a write to the accelerometer with the appropriate read operation and response from the accelerometer.

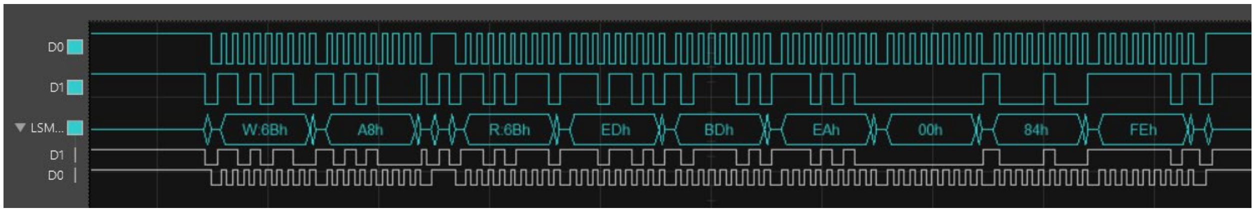

Figure 4.6. I^2C Sensor Data Transfer

Next, two tests were employed to verify that the Cypress CYW20719 microcontroller and the selected sensor packages were capable of satisfying the Data Display constraint. The first of these tests began reading information from the sensors as fast as the microcontroller would allow and counted the total number of complete sensor frames read during a three second period. The second test, in comparison, measured the period of time required to read a constant number of sensor frames. These two tests yielded similar results and are shown in Table 4.3.

Table 4.3. Sensor Polling Tests

Test	**Minimum Required**	**Actual**
Total # of Readings in 3 seconds	>= 360 frames (120 frames/sec)	4470 frames (1490 frames/sec)
Time to read 10000 sensor frames	<= 83.3 sec (120 frames/sec)	7 seconds (1428.6 frames/sec)

The slower measured polling rate, 1428.6 frames per second, is over 10 times faster than required by the Data Display constraint.

4.2.3. Bluetooth Broadcast

The data throughput capabilities of the Bluetooth communication system were also tested against the Data Display constraints. For this test, the Cypress CYW20719 microcontroller was configured to transmit one 56-byte frame every 8 ms (125 Hz) to the coaching application. Upon reception of the frame by the coaching application, the current time was recorded. The time differences were computed for a few seconds of data. Figure 4.7 shows data frames being received in bursts by the coaching application. These bursts are caused by context switching and Bluetooth buffering of the operating system. However, these bursts do not affect the expected average throughput, which exceeds the design constraint of 120 Hz.

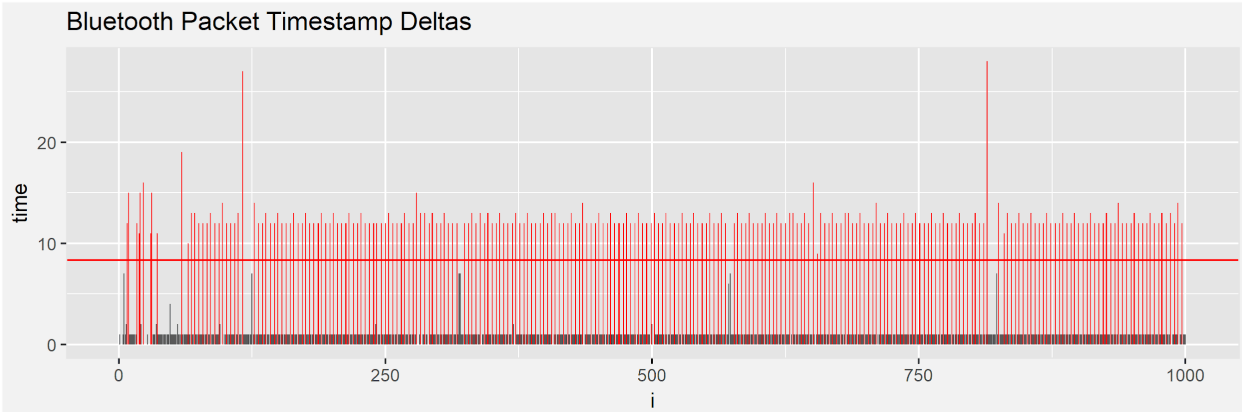

Figure 4.7. Bluetooth Broadcast Test

4.2.4. Hardware Footprint

The Golf Glove system main footprint consists of a Cypress CYW20719 microcontroller and four Analog to Digital Converters (ADC). These two components can be seen in Figure 4.8 and Figure 4.9. In Figure 4.8, the microcontroller and support circuitry are indicated by the red square, approximately 18 mm x 18 mm in size.

Figure 4.8. Microcontroller and Support Circuitry

In Figure 4.9, the four ADCs are indicated by the red squares. Each ADC is 3 mm x 4 mm.

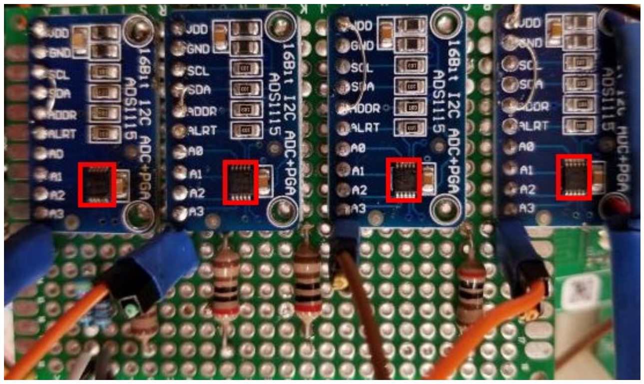

Figure 4.9

With a combined area of 372 mm^2, the main components are well within our design constraint of 1935.48 mm^2.

4.3. Coaching Application Subsystem

4.3.1. Bluetooth Reception

The Wireless Communication constraint requires that Golf Glove maintains Bluetooth communication at distances up to 9.15 meters. To test that the Golf Glove's microcontroller satisfies this constraint, firmware that continuously broadcasts data was loaded onto the CYW20719 development board. Using Cypress' CySmart application on a mobile phone, the RSSI of this broadcast was measured at 1 meter increments up to 15 meters. The graph of RSSI over distance is charted below in Figure 4.10. A signal strength of approximately -67 dBm was measured at 9.15 m.

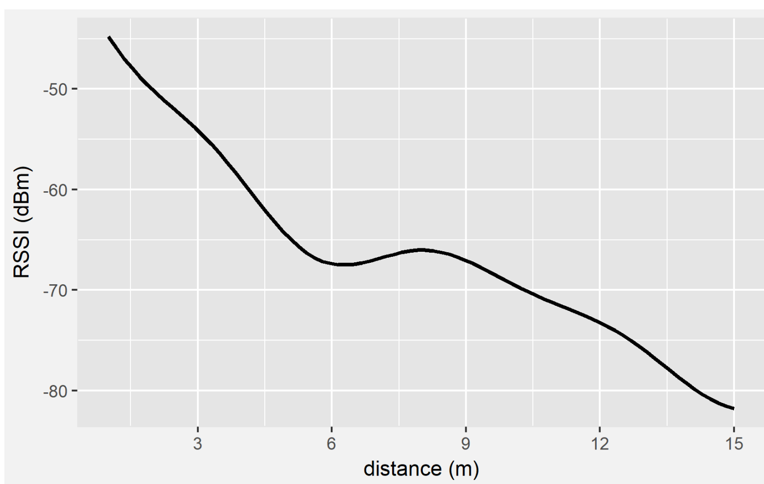

Figure 4.10. RSSI of Golf Glove Broadcast

4.3.2. Database

On the backend of the coaching application, the data must be stored as quickly as it is received to prevent a buffer overflow. Following the Data Display constraint, the write performance of the database must be at least 120 Hz. To test its performance, the coaching application backend wrote 500 data frames to the SQLite database and recorded the timestamp deltas between inserts. All timestamp deltas satisfied the design constraint with an average write performance over 1.3 kHz. Figure 4.11 shows the timestamp deltas for each frame.

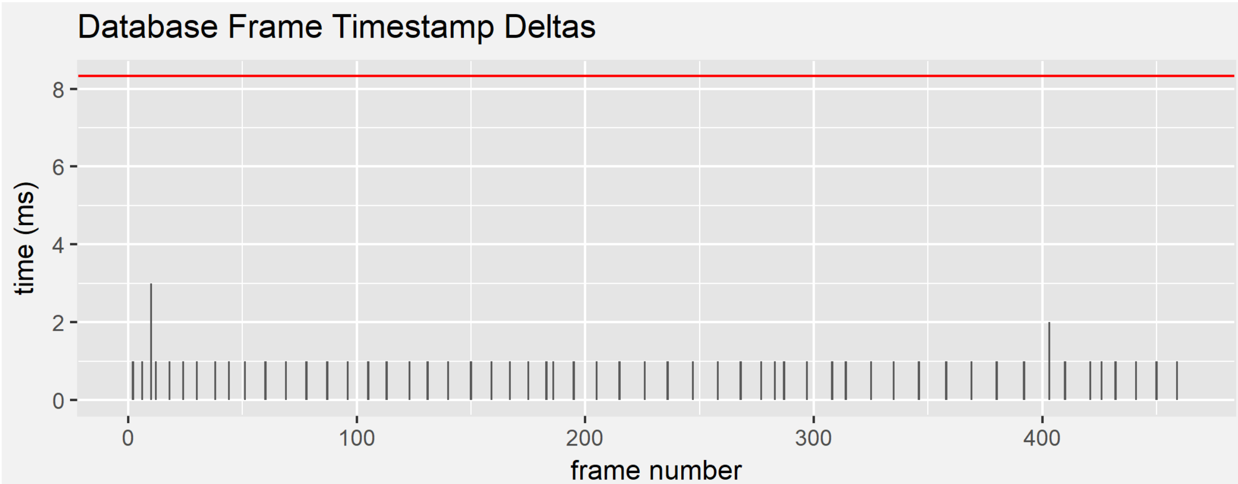

Figure 4.11. Frame-to-frame delay for 500 frames

4.3.3. WebSocket Bandwidth

Meanwhile, the coaching application is also sending sensor frames to the frontend for display. The backend-to-frontend communication speed must exceed 120 Hz to support the Data Display constraint. To test the backend-to-frontend throughput, the backend sent 10,000 frames while the frontend recorded the time deltas upon reception of the frame. Figure 4.12 is a graph of the timestamp deltas. The values outlined in red do not meet the constraint delta. Similar to the Bluetooth Throughput test though, this is a consequence of protocol buffering. The application averages 0.6 ms (1.6 kHz) between each data frame, more than 10 times faster than the Data Display constraint.

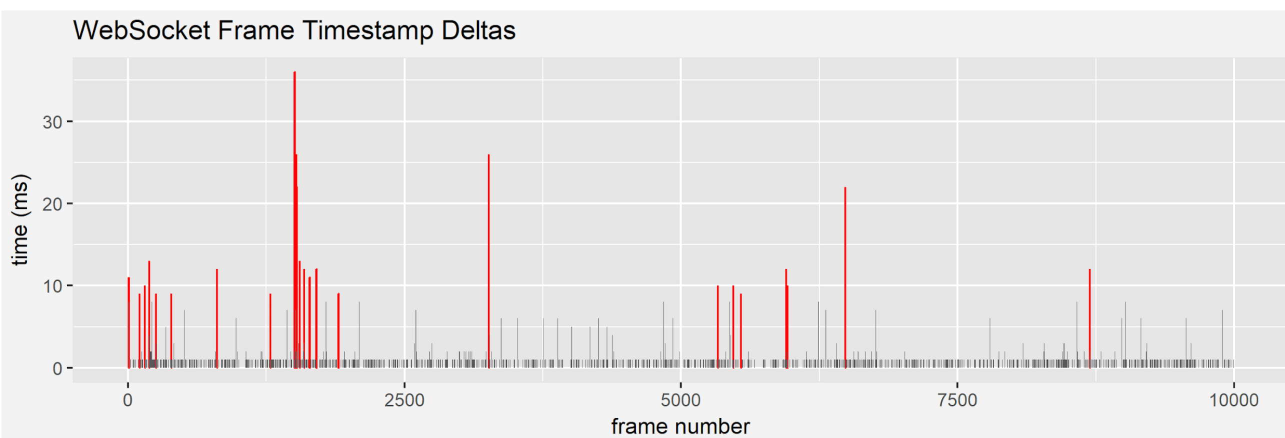

Figure 4.12. Frame-to-frame delay for 10,000 frames

4.4. Integrated System

To complete the integrated system test, the wrist-mounted controller and the coaching application were first powered on. Next, the frontend instructed the backend to connect to the glove. The coaching application successfully connected to the Golf Glove at a distance of 10 m, satisfying the Wireless Communication constraint. Sensor data began streaming to the coaching application and the distance was increased to 48 m. During the test, the wrist-mounted controller remained connected and data was received on the front-end at a rate of at least 120 Hz, satisfying the Data Display constraint. Figure 4.13 and Figure 4.14 show the two components of the integrated system test.

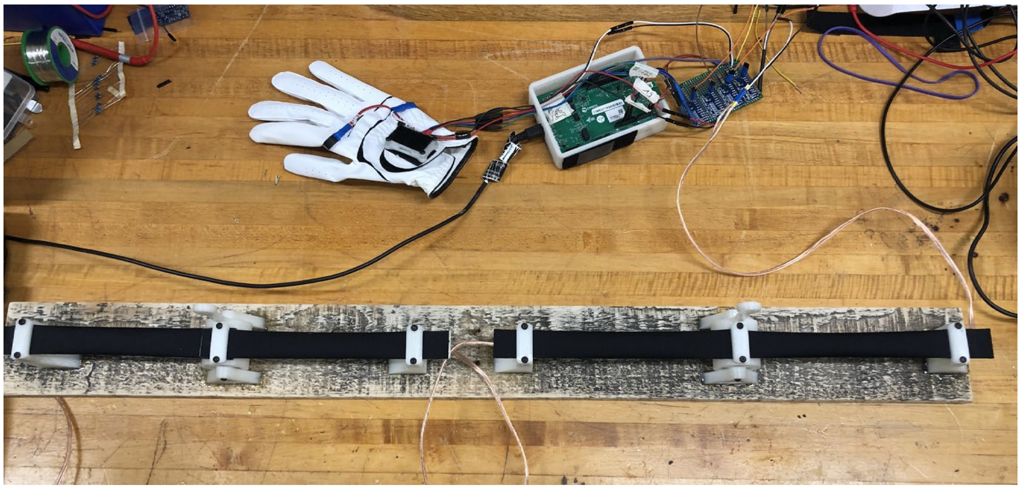

Figure 4.13. The glove and wrist-mounted controller

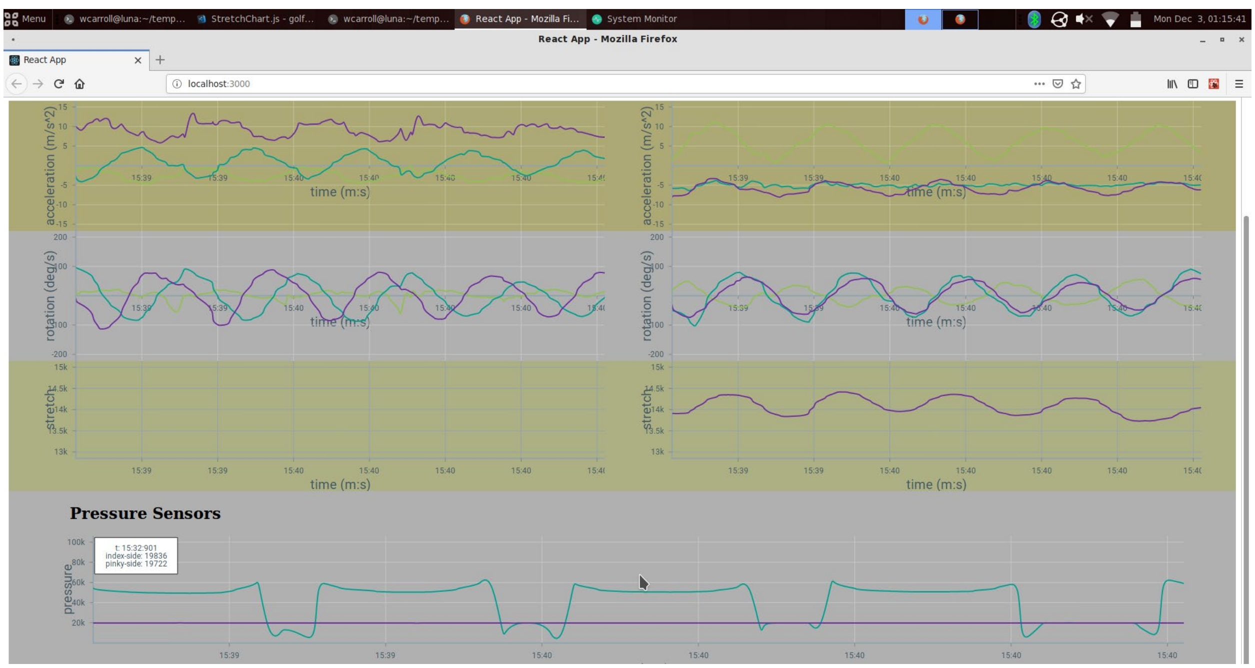

Figure 4.14. The coaching application display

Table 4.4 is a summary of the tests performed in Golf Glove's evaluation. All tests passed and the system surpassed expectations.

Table 4.4: Summary of Tests

Technical Constraints	**Test Results**
Hand Orientation	LiquidWire measured to have linear relationship between resistance and stretch, and accuracy measured within 3°. Accelerometer and gyroscope measured to within 5% margin of error.
Wireless Communication	Wireless communication tested greater than 9.15 m.
Data Display	WebSockets tested to achieve greater than 120 Hz.
Unobtrusive	With a combined area of 3.72 cm^2, the main components fit within an area of 19.35 cm^2.
Portability	Battery was able to successfully supply enough capacity to power the device for a minimum of 5 hours.

5. SUMMARY AND FUTURE WORK

Throughout the design process, several problems were encountered. The problems that impacted the overall design are broken down by hardware, microcontroller, and coaching application sections. The current system records inertial, pressure, and stretch sensors. The design is currently limited by a cumbersome development board and by stretch sensor mounting difficulties. Future developments involving the Golf Glove system are discussed below.

5.1. Hardware

The design initially used the integrated ADCs on the Cypress CYW20719 chip to poll the LiquidWire and pressure sensors. Due to the low change in resistance between the resting and stretched states of LiquidWire sensors, programmable gain amplifiers are necessary. To mitigate this problem, a Texas Instruments ADS1115 16-bit ADC was selected, predicting that it would allow four LiquidWire sensor readings simultaneously. An issue arose from this solution: the ADS1115 contains only one internal ADC and switches between each analog input to complete conversions. This switching introduced a delay into the system that prevented the glove from reading all sensors simultaneously and was too slow to meet speed constraints. To solve this problem, three additional ADCs were added to the design.

More issues arose when upon mounting the stretch sensors on the wrist-mounted unit. LiquidWire's stretch sensors must remain taut to output useful data to the glove. Any amount of slack in the sensors results in inaccurate and unusable resistance values. The initial design required attaching a strap on the wrist-mounted controller that could be tightened around the user's wrist. When the user tightens the wrist unit such that the LiquidWire sensors are held taut, the tightened strap becomes uncomfortable and hinders the movement of the user. The design was modified to use a compression sleeve outfitted with internal rubber to provide adequate friction around the arm and keep the wrist-mounted controller stationary. Unfortunately, the sleeve did not prevent sliding of the wrist-mounted controller, loosened the LiquidWire, and compromised the data gathered from the sensors.

5.2. Microcontroller

The Cypress CYW20719 microcontroller also required specific initialization for system data types and functions such as threading, timers, and queues. Initially, the team was unfamiliar with the syntax of using these functions. Cypress BLE chips are a relatively new product for the company and thus the documentation was lacking. After contacting Cypress Customer Support, the team was provided with example code explaining the syntax and functionality of these resources in the Real-Time Operating System.

Also, in order to conserve memory and processing power, the microcontroller doesn't support floating-point arithmetic. Originally, the firmware intended to handle data parsing such as converting I^2C reads from unsigned 8-bit integers to float objects; however, due to the restriction on the microcontroller, data parsing and formatting code was moved to the backend server of the coaching application.

5.3. Coaching Application

During development, the team quickly found there were dependency issues preventing Bluetooth reception. The main issue occurred between *noble* (the Bluetooth framework chosen in the Approach) and *Electron* (the desktop environment used for rendering the GUI) were incompatible. To resolve this compatibility issue, the frontend GUI was changed to simply render the data in an internet browser. This change required creating an HTTP server to communicate the sensor frames from the backend to the frontend as this architecture requires two separate processes to run noble and the frontend rendering. WebSockets were chosen as the backend to frontend communication protocol to allow the backend to push data to the frontend without explicit requests for data from the frontend.

5.4. Future Features

The Golf Glove firmware currently exposes raw sensor values to the coaching application in real-time mode, allowing for any application that can interface with BLE to connect and read sensor values. One future application could add an RFID sensor to the glove to detect golf club type with special RFID tags embedded in the club handle. Swing detection characteristics could be modified based on the club type to enable detection of different swing types such as chipping or putting.

The Golf Glove could also pair with a golf scoring application to record swings and golf scores in a database. Once many swings across multiple rounds of golf are recorded, a machine learning algorithm could be used to identify common characteristics of successful golf swing technique as well as common swing mistakes.

6. ACKNOWLEDGEMENTS

The Golf Glove team would like to thank the following people:

Dr. John Ball, Assistant Professor in the Electrical and Computer Engineering Department at Mississippi State University, for providing initial introductions to the athletic department and his support of our project.

Tony Luczak, Graduate Research Assistant in the Recreational Sports Department at Mississippi State University, for providing expert advice in golf technique and business modeling.

7. REFERENCES

[1] "History of Golf," International Golf Federation. [Online]. Available: https://www.igfgolf.org/about-golf/history. [Accessed: 13-Sep-2018].

[2] R. Neal, "3D Kinematics and Kinetics of the Golf Swing," *International Journal of Sport Biomechanics*, 1985. [Online]. Available: https://journals.humankinetics.com/doi/abs/10.1123/ijsb.1.3.221. [Accessed: 12-Sep-2018]

[3] A. Josephson, "The Economics of Golf," *SmartAsset*, 2018. [Online]. Available: https://smartasset.com/retirement/the-economics-of-golf. [Accessed: 03-Sep-2018].

[4] "Pricing | Topgolf Allen," *Topgolf*. [Online]. Available: https://topgolf.com/us/allen/pricing/. [Accessed: 04-Sep-2018].

[5] D. Johnson, "Best golf swing analyzers and shot trackers," *Gadgets & Wearables*, 22-Apr-2018. [Online]. Available: https://gadgetsandwearables.com/2018/04/22/golf-swing-analyzer. [Accessed: 04-Sep-2018].

[6] "Standard Lengths," *GolfWorks*. [Online]. Available: https://www.golfworks.com/images/art/StdLengths.pdf. [Accessed: 23-Sep-2018].

[7] "Driver-Head-Shapes and dimensions," *Cast irons and Forged Irons, Manufacturing and Materials*. [Online]. Available: http://www.golfclub-technology.com/driver-head-shapes.html. [Accessed: 23-Sep-2018].

[8] "Average Golf Swing Speed Chart," *Swing Man Golf – Blog*, 22-May-2018. [Online]. Available: http://www.swingmangolf.com/average-golf-swing-speed-chart-2/. [Accessed: 23-Sep-2018].

[9] J. Brauer, "Practical Tee Design," *Golf Course Industry*, 08-Aug-2006. [Online]. Available: http://www.golfcourseindustry.com/article/practical-tee-design--design-column-/. [Accessed: 05-Oct-2018].

[10] C. Wang, "Hand tool handle design based on hand measurements," MATEC Web Conf. [Online]. Available: https://www.matec-conferences.org/articles/matecconf/pdf/2017/33/matecconf_imeti2017_01044.pdf [Accessed: 24-Sep-2018].

[11] L. Vorvick, "Calculating body frame size: MedlinePlus Medical Encyclopedia Image," *MedlinePlus*, 13-Jul-2016. [Online]. Available: https://medlineplus.gov/ency/imagepages/17182.htm. [Accessed: 24-Sep-2018].

[12] Cole, M. H., & Grimshaw, P. N. (2016). The biomechanics of the modern golf swing: implications for lower back injuries. *Sports Medicine*, *46*(3), 339-351.

[13] B. Kelley, "How Long Does It Take to Play a Round of Golf?," *ThoughtCo*. [Online]. Available: https://www.thoughtco.com/time-it-takes-to-play-a-round-1560498. [Accessed: 24-Sep-2018].

[14] "Lithium Polymer Charging/Discharging & Safety Information," *MaxAmps.com*. [Online]. Available: https://www.maxamps.com/lipo-care.php. [Accessed: 24-Sep-2018].

[15] Secure Systems and Technologies. (2018). *Ingress Protection*. [Online] Available at: http://sst.ws/downloads/Ingress-Protection-iss-4.pdf [Accessed 19 Sep. 2018].

[16] RoHSguide.com, RoHS Guide. http://www.rohsguide.com/rohs-faq.htm. [Accessed: 27-Sep-2018]

[17] Standard, I. E. C. 62209-2: Human Exposure to Radio Frequency Fields From Hand-Held and Body-Mounted Wireless Communication Devices Human Models. Instrumentation, and Procedures—Part, 1. [Accessed: 25-Sep-2018].

[18] Directive, R. (2003). Directive 2002/95/EC of the European Parliament and of the Council of 27 January 2003 on the restriction of the use of certain hazardous substances in electrical and electronic equipment. Official Journal of the European Union, 13, L37.

[19] Ahlbom, A., Bergqvist, U., Bernhardt, J. H., Cesarini, J. P., Grandolfo, M., Hietanen, M., ... & Swicord, M. L. (1998). Guidelines for limiting exposure to time-varying electric, magnetic, and electromagnetic fields (up to 300 GHz). Health physics, 74(4), 494-521.

[20] “Liquid Wire Technology,” Liquid Wire. [Online]. Available: https://liquidwire.io/technology. [Accessed: 26-Oct-2018].

[21] “Hand Grip Strength: age and gender stratified normative data in a population-based study,” BMC Res Notes, Apr. 2011.

[22] E. Komi, J. Roberts, and S. Rothberg, “Measurement and analysis of grip force during a golf shot,” Proceedings of the Institution of Mechanical Engineers Part P Journal of Sports Engineering and Technology, Jun. 2008.

[23] “FS R ® 400 Series Data Sheet,” 2017. [Online]. Available: https://cdn2.hubspot.net/hubfs/3899023/Interlinkelectronics November2017/Docs/Datasheet_FSR.pdf. [Accessed: 25-Oct-2018].

[24] Adafruit Industries, “Pressure-Sensitive Conductive Sheet (Velostat/Linqstat),” adafruit industries blog RSS. [Online]. Available: https://www.adafruit.com/product/1361. [Accessed: 26-Oct-2018].

[25] “Acceleration,” Quintic Sports. [Online]. Available: https://www.quinticsports.com/wp-content/uploads/2016/06/Case-Study-12-Acceleration.pdf. [Accessed: 25-Oct-2018].

[26] Loopy, “Golf Swing Sequence and Timing – The Downswing,” Golf Loopy - Play Your Golf Like a Champion, 14-Oct-2015. [Online]. Available: http://www.golfloopy.com/golf-swing-sequence-and-timing-downswing/. [Accessed: 25-Oct-2018].

[27] “LSM9DS1 Datasheet.” [Online]. Available: https://www.st.com/resource/en/datasheet/lsm9ds1.pdf. [Accessed: 25-Oct-2018].

[28] “Bosch Sensortec BMX055 Datasheet.” [Online]. Available: https://ae-bst.resource.bosch.com/media/_tech/media/datasheets/BST-BMX055-DS000-02.pdf. [Accessed: 25-Oct-2018].

[29] “mCube MC6479 Preliminary Datasheet.” [Online]. Available: https://www.mouser.com/datasheet/2/693/MC6470-Preliminary-Datasheet-APS-048-0033v1.6--1489118.pdf. [Accessed: 25-Oct-2018].

[30] “Enhanced Low Power, BR/EDR/BLE Bluetooth 5.0 SOC Datasheet,” 12-Jul-2018. [Online]. Available: http://www.cypress.com/file/414181/download. [Accessed: 25-Oct-2018].

[31] “Bluetooth® Low Energy (BLE) SoC.” [Online]. Available: http://ww1.microchip.com/downloads/en/DeviceDoc/IS1870_71-Bluetooth-Low-Energy-BLE-SoC-DS60001371E.pdf. [Accessed: 25-Oct-2018].

[32] “Li-Polymer Battery Technology Specification,” Adafruit Industries. [Online]. Available: https://cdn-shop.adafruit.com/product-files/1578/C1854 PKCell Datasheet Li-Polymer 503035 500mAh 3.7V with PCM.pdf. [Accessed: 25-Oct-2018].

[33] “Robot?,” Newegg- Computer Parts, Laptops, Electronics, HDTVs, Digital Cameras and More![Online]. Available: https://www.newegg.com/Product/Product.aspx?Item=9SIA4SR6YH7231&ignorebbr=1&nm_mc=KNC-GoogleMKP-PC&cm_mmc=KNC-GoogleMKP-PC-_-pla-_-AT - Batteries & Accessories - Replacement-_-

9SIA4SR6YH7231&gclid=Cj0KCQjw08XeBRC0ARIsAP_gaQBDs4SNdrioxPFeVZ5y1T08FjWVodO-wwc_uowzROIrS8EiuxSbWOAaAlTUEALw_wcB&gclsrc=aw.ds. [Accessed: 26-Oct-2018].

[34] "MX2400 Alkaline-Manganese Dioxide Battery Datasheet." [Online]. Available: http://professional.duracell.com/downloads/datasheets/product/Ultra Power/Ultra-Power_AAA_MX2400.pdf. [Accessed: 25-Oct-2018].

[35] "Manganese Dioxide Lithium Coin Batteries: Individual Specifications." [Online]. Available: https://www.alliedelec.com/m/d/6ec5c9a8833414eb34f877f612fc890f.pdf. [Accessed: 25-Oct-2018].

[36] "noble/noble," GitHub, 08-Jun-2018. [Online]. Available: https://github.com/noble/noble. [Accessed: 26-Sep-2018].

[37] "Electron," Electron. [Online]. Available: https://electronjs.org/. [Accessed: 26-Sep-2018].

[38] "React – A JavaScript library for building user interfaces," React. [Online]. Available: https://reactjs.org/. [Accessed: 26-Sep-2018].

8. APPENDIX: PRODUCT SPECIFICATION